ENVIRONMENTAL CONTROL OF CLOUD-TO-GROUND LIGHTNING POLARITY IN SEVERE STORMS DURING IHOP

Lawrence D. Carey* and Kurt M. Buffalo
Texas A&M University, College Station, Texas

1. INTRODUCTION

The overwhelming majority of severe storms throughout the contiguous United States generate primarily (> 75%) negative ground flashes (so-called negative storms). However, a certain subset of severe storms produces an anomalously high (> 25%) percentage of positive ground flashes (so-called positive storms). The frequency of these "anomalous" positive storms varies regionally and seasonally. In some regions (e.g., central and northern plains) and months, these positive storms are common, representing 30% or more of all severe storms (Carey et al. 2003; Carey and Rutledge 2003).

Several past studies have noted that severe storms passing through similar mesoscale regions on a given day exhibit similar CG lightning behavior (Branick and Doswell 1992; MacGorman and Burgess 1994; Smith et al. 2000). This repeated observation led to the hypothesis that the local mesoscale environment indirectly influences CG lightning polarity by directly controlling storm structure, dynamics, and microphysics, which in turn control storm electrification (e.g., MacGorman and Burgess 1994). *According to one hypothesis, intense updrafts and associated high liquid water contents in positive storms lead to positive charging of graupel and hail via the non-inductive charging mechanism* (e.g., Takahashi 1978; Saunders et al 1991), *an enhanced lower positive charge, and increased frequency of positive CG lightning* (e.g., MacGorman and Burgess 1994; Carey and Rutledge 1998; Gilmore and Wicker 2002). A handful of studies have explored the detailed relationship between the mesoscale environment and the CG lightning behavior of severe storms (Reap and MacGorman 1989; Curran and Rust 1992; Smith et al. 2000; Gilmore and Wicker 2002). Smith et al. (2000) found that *positive* (negative) storms occurred in a *strong* (weak) gradient region of the surface equivalent potential temperature (θ_e), *upstream* (over or downstream) of a θ_e maximum or ridge. Gilmore and Wicker (2002) found that boundary crossing supercells transitioned from dominant negative to dominant positive CG lightning when the storms experienced enhanced CAPE and low-level vertical wind shear on the immediate cool side of the boundary. Since it is difficult to obtain representative inflow soundings, only a few studies have analyzed mesoscale environmental characteristics in conjunction with CG lightning properties. Clearly, further study is warranted.

* *Corresponding author address*: Dr. Larry Carey, Dept. Atmospheric Sciences, Texas A&M University, College Station Texas 77843-3150; larry_carey@tamu.edu

This study seeks to investigate the relationship between positive CG dominant storms and the immediate meteorological environment in which they occur, thereby providing further insight into why only some severe storms are dominated by positive CG flashes, and in particular, what conditions lead to this positive CG dominance. A determination of whether environmental conditions are systematically related to positive CG production by severe storms, and if so, what these conditions are, is a crucial step in determining the reliability of using NLDN real-time flash polarity data for nowcasting. Furthermore, determining the relationship between certain environmental conditions and positive severe storms will lead to an improved understanding of the cloud electrification mechanisms at work in these storms, which remains speculative at this time (e.g., MacGorman and Burgess 1994; Carey and Rutledge 1998; Smith et al. 2000; Williams 2001; Gilmore and Wicker 2002, Carey et al. 2003; Lang et al. 2004).

Using data from the International H_2O Project (IHOP-2002), we have found clear, systematic differences between the mean mesoscale environments associated with positive storms (4 regions) and negative storms (5 regions) (Carey and Buffalo 2004). In particular, positive mesoscale regions were characterized by a higher mean lifting condensation level (LCL), smaller mean warm cloud depth (i.e., height of freezing level – height of LCL), larger mean CAPE (Convective Available Potential Energy) from -10°C to -40°C, larger mean NCAPE (Normalized CAPE) from LFC to -40°C, larger 0-3 km mean shear, and larger 0-2 km mean storm-relative wind speed (Carey and Buffalo 2004). According to well known principals of dynamics and microphysics, each of these significant differences in the mean mesoscale environment could contribute to stronger updrafts and/or higher liquid water contents in the mixed-phase zone of positive storms (Bluestein 1993; Houze 1993) and hence positive charging of graupel and hail, an enhanced lower positive charge, and dominant positive CG production.

In this follow-on paper to Carey and Buffalo (2004), we investigate the detailed environmental conditions of two positive storms that occurred during IHOP on 24 May and 19 June 2002, during which aircraft-released dropsondes measured the high-resolution horizontal and vertical structure of the environment. The dropsonde lines were roughly perpendicular to the surface θ_e ridge and low-level boundary associated with convective initiation and roughly parallel to subsequent storm motion, allowing us to extend the results of Carey

and Buffalo (2004), Gilmore and Wicker (2002), and Smith et al. (2000).

a.

b.

Figure 1. Convective initiation (CI) mission summaries for **a)** 24 May 2002 and **b)** 19 June 2002 during IHOP. The Learjet released GPS dropsondes at points (purple triangles) every 20 km to 30 km along a line roughly perpendicular to a low level boundary. See http://www.ofps.ucar.edu/ihop/catalog/missions.html for more details.

2. DATA AND METHODOLOGY

A line of GPS dropsondes were released on both 24 May (Figure1a) and 19 June 2002 (Figure 1b) from the Flight International Learjet during IHOP-2002. The lines were roughly perpendicular to low level boundaries associated with convective initiation (CI) and approximately parallel to subsequent storm motion (Figures 1a,b). Once the location of CI is accounted for, these dropsondes are excellent proximity environmental soundings that are likely representative of inflow conditions for storms occurring on each day. The lines of dropsondes were oriented roughly perpendicular to the θ_e ridge on each respective day (not shown), permitting investigation of the vertical structure of the θ_e gradient region, which has been found to be a preferred location for the occurrence of positive storms (e.g., Smith et al. 2000; Carey et al. 2003).

On 24 May 2002, nine dropsondes were released between 2022 and 2046 UTC, with a time interval between each release of 3 minutes, resulting in an average distance between dropsonde locations of approximately 27 km. The dropsondes were released from roughly 4 km AGL. Seven of the nine dropsondes contained good data and could be used for analysis. Eight dropsondes were released on 19 June 2002 between the times of 2110 and 2131 UTC, with each release separated by a time step of 3 minutes and distance of approximately 24 km. These dropsondes were released from roughly 5.5 km AGL. All eight of the 19 June dropsondes were used for analysis.

Parameters investigated with the dropsonde data include LCL heights, CAPE, NCAPE, depth of the warm cloud layer, freezing level heights, and 0-3 km vertical wind shear. All heights are above ground level (AGL) unless otherwise stated. For the 24 May case, any vertical levels at pressures less than 575 mb were removed from the dropsonde data files, since 575 mb was the lowest pressure (greatest height) level measured by all dropsondes. This process ensured that NCAPE was calculated through the same vertical level for all dropsondes within the dropsonde line, thereby allowing for more equal comparisons of NCAPE between all dropsondes in the line. Similarly, any vertical levels at pressures less than 455 mb were removed from the 19 June dropsonde data files.

The National centers Advanced Weather Interactive Processing System (NAWIPS) Skew-T Hodograph Analysis and Research Program (NSHARP) was used for sounding display and analysis. NSHARP includes a virtual temperature correction for thermodynamic calculations (e.g., Doswell and Rasmussen 1994). A mean-layer parcel (using mean temperature and dew point in the lowest 100 hPa) was used to calculate thermodynamic parameters, since a mean-layer parcel is likely more representative of the actual parcel associated with convective cloud development than is a surface-based parcel (Craven et al. 2002).

Vertical cross-sections of parcel buoyancy (B),
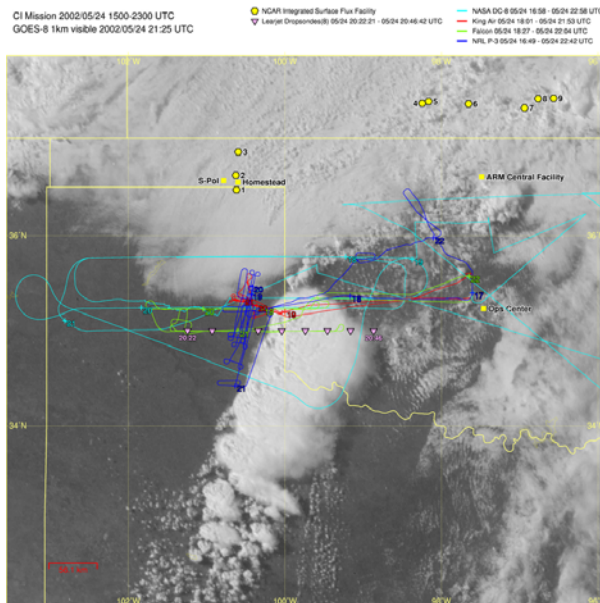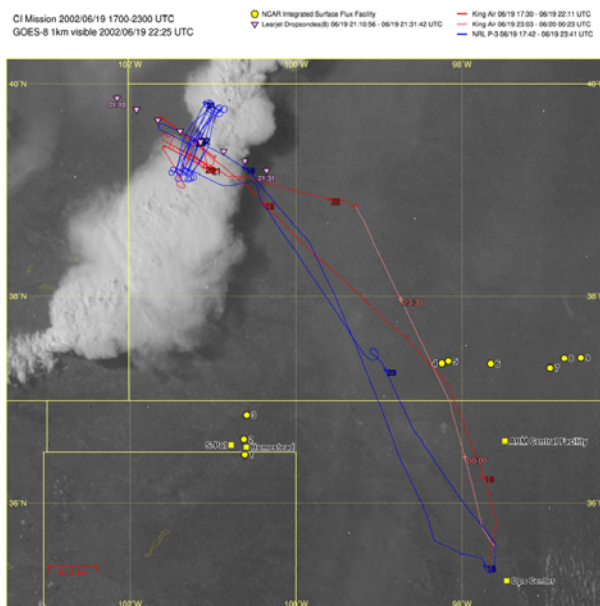
$$B = g\left(\frac{T_v(z) - \overline{T}_v(z)}{\overline{T}_v(z)}\right) \quad (1)$$

where $T_v(z)$ and $\overline{T}_v(z)$ are the parcel and environmental virtual temperatures, respectively, at a given height (z) were created along the Learjet flight path on 24 May and 19 June 2002 from the dropsonde data. A FORTRAN program (Emanuel 1994) was used to calculate B at each vertical level (every 5 mb) for each dropsonde using the mean temperature and dewpoint in the lowest 100 hPa and assuming pseudoadiabatic ascent. This process resulted in a vertical buoyancy profile for each dropsonde location.

An IDL (Interactive Data Language) program was developed that used these vertical buoyancy profiles at each dropsonde location to create vertical cross-sections of buoyancy along the two dropsonde lines. The buoyancy values at each dropsonde location were used to create a regular grid of interpolated buoyancy values, and then these regularly-gridded buoyancy values were contoured. The buoyancy data were interpolated by using the "IRREGULAR" keyword with IDL's "CONTOUR" procedure, which performs a Delaunay triangulation to interpolate irregularly-gridded data to a regular grid. The vertical cross-sections of buoyancy were used to investigate the distribution of buoyancy (both horizontally and vertically) in the θ_e gradient region. The buoyancy cross-sections were also used to assess the magnitude of horizontal vorticity produced by the horizontal buoyancy gradients (dB/dH) (i.e., baroclinic generation of vorticity) in the θ_e gradient region, since the tilting of this horizontal vorticity into the vertical by a storm updraft can lead to the development of nonlinear dynamic pressure perturbations, and associated increases in updraft intensity (Rasmussen et al. 2000; Gilmore and Wicker 2002; Carey et al. 2003).

## 3. RESULTS

3.1 NLDN and WSR-88D composite behavior

As shown in Figure 2a, CG lightning polarity on 24 May 2002 over the IHOP domain transitioned from positive in western Oklahoma/Texas (mean positive CG percentage = 32% in the red box) to negative in central Oklahoma/Kansas (mean positive CG percentage = 8% in the blue box). By contrast, positive storms (mean positive CG percentage = 72% in the red box) were ubiquitous over Kansas and Nebraska on 19 June 2002 (Figure 2b).

Positive storm cells on 24 May in the western IHOP domain were both ordinary and, in several cases, supercells embedded within a larger squall line (Figure 3a). The squall line weakened and became more broken in areal coverage as it moved eastward to central Oklahoma and Kansas (Figure 3b). The negative storm cells embedded within the weakened squall line in the eastern IHOP domain were entirely ordinary. Both negative and positive storms were severe over the IHOP domain on 24 May 2002.

On 19 June, convection was primarily organized as a broken squall line comprised of ordinary but intense and severe cells over Kansas and Nebraska (Figure 4a). An isolated tornadic supercell developed to the rear (i.e., westward) of the eastward moving broken squall line along its outflow boundary (Figure 4a). It is important to note that all of the convection, regardless of cell type, generated a high percentage of positive CG lightning on 19 June 2002 (c.f. Figures 2b, 4a,b).

a.

b.
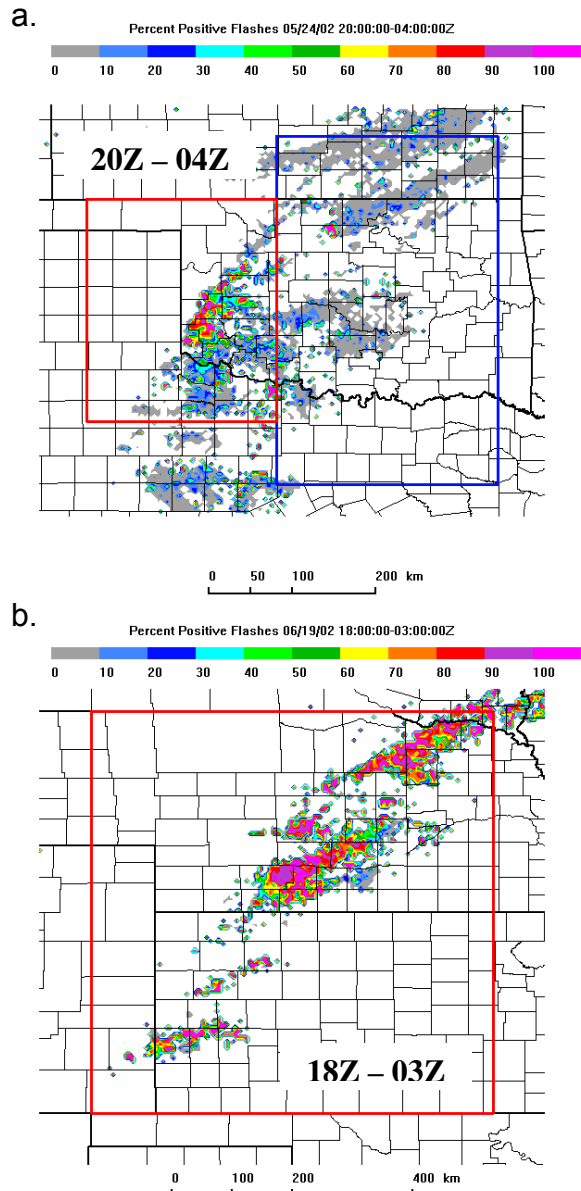
Figure 2. The percentage (%) of positive ground flashes on **a)** 24 May 2002 from 24/18Z to 25/00Z and **b)** 19 June 2002 from 19/18Z – 20/03Z. A red (blue) box indicates a mesoscale region associated with positive (negative) storms. State and county boundaries are shown. Horizontal distance is indicated by the key at the bottom of each figure.
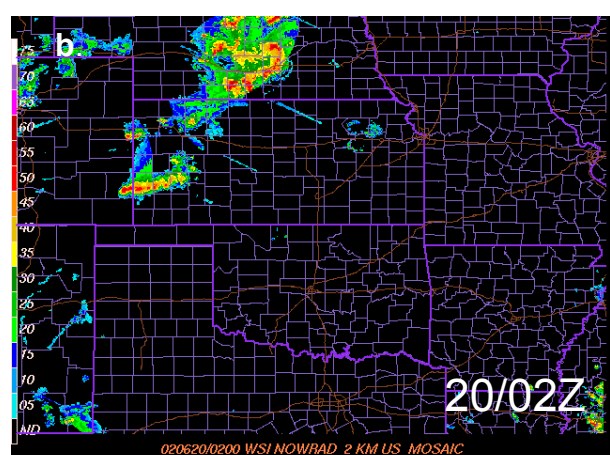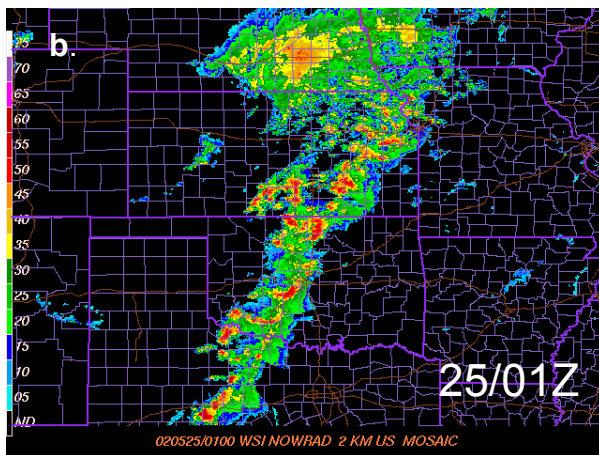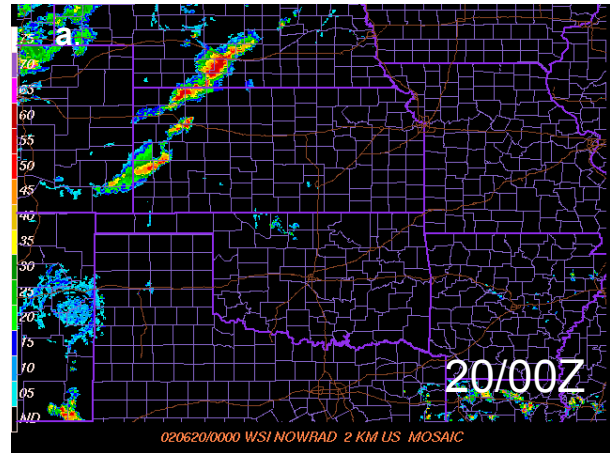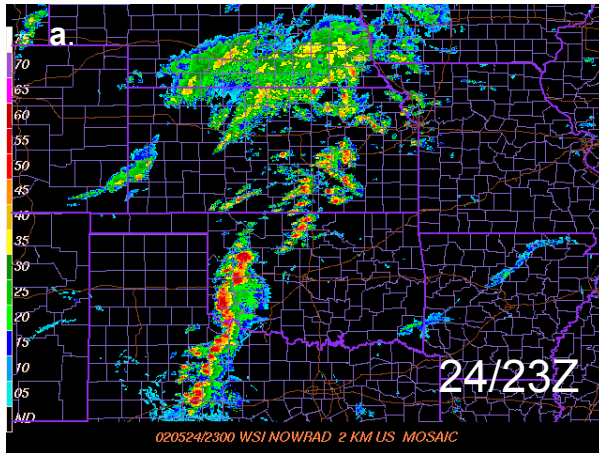
Figure 3. WSI NOWRAD mosaic of low-level WSR-88D reflectivity structure over the IHOP domain on 24 May 2002 at **a)** 24/23Z and **b)** 25/01Z.

Figure 4. Same as Figure 3 except for 19 June 2002 at **a)** 20/00Z and **b)** 20/02Z.

### 3.2 Dropsonde derived environmental parameters

The horizontal structure of thermodynamic parameters (NCAPE, warm cloud depth, LCL, freezing level) and low-level (0-3 km) wind shear that were calculated from the 24 May and 19 June dropsondes along the Learjet flight track are shown in Figures 5 and 6, respectively. On 24 May, a cold front was located between the second and third dropsondes (2025Z sonde around 30 km and 2031Z sonde around 80 km in Figure 5). There was also a dryline intersecting the cold front, forming a triple point in the vicinity of the Learjet flight track. The dryline ran between the third and fourth dropsondes (2031Z and 2034Z sonde near 110 km), which is where CI occurred (Figure 5). On 19 June, a weak cold front was located between the fifth and sixth dropsondes (2122Z sonde around 100 km and 2125Z sonde around 125 km), and CI occurred right ahead of and along the front (Figure 6).

On 24 May 2002, NCAPE rapidly increased in the vicinity of the dryline, where convection initiated, and peaked at about 0.11 m s^{-2} just 10-40 km eastward into the warmer and moister air (Figure 5a). Although low-level shear was stronger rearward (i.e., westward) of the

dryline and cold front, a relative maxima in the 0-3 km shear (17.5 m s^{-1}) was located just east of the dryline at 110 km (Figure 5a). As a result, the developing convection on 24 May experienced initially increasing and near peak values of NCAPE and low-level shear. The positive CG percentage also rapidly increased eastward of the dryline to a maximum value of 73% at a point centered just 35 km eastward (i.e., at 135 km along the Learjet flight track) likely in response to these elevated values of NCAPE and low-level shear. Moving further eastward, the NCAPE decreased dramatically (up to 36%) and the low-level shear dropped slightly. At the same time, the positive CG percentage also decreased significantly from the peak of 73% to only 24%, which is just below the subjective threshold required for positive storm status. The height of the LCL peaked just 20 km westward of the dryline (Figure 5b). Initial convection on 24 May was associated with an LCL between the maximum of 2200 m and 1600 m, which was measured just 10 km eastward of the dryline where convection initiated (i.e., 110 km along the Learjet flight track). The LCL continued to decrease eastward, reaching 1000 m at the last dropsonde
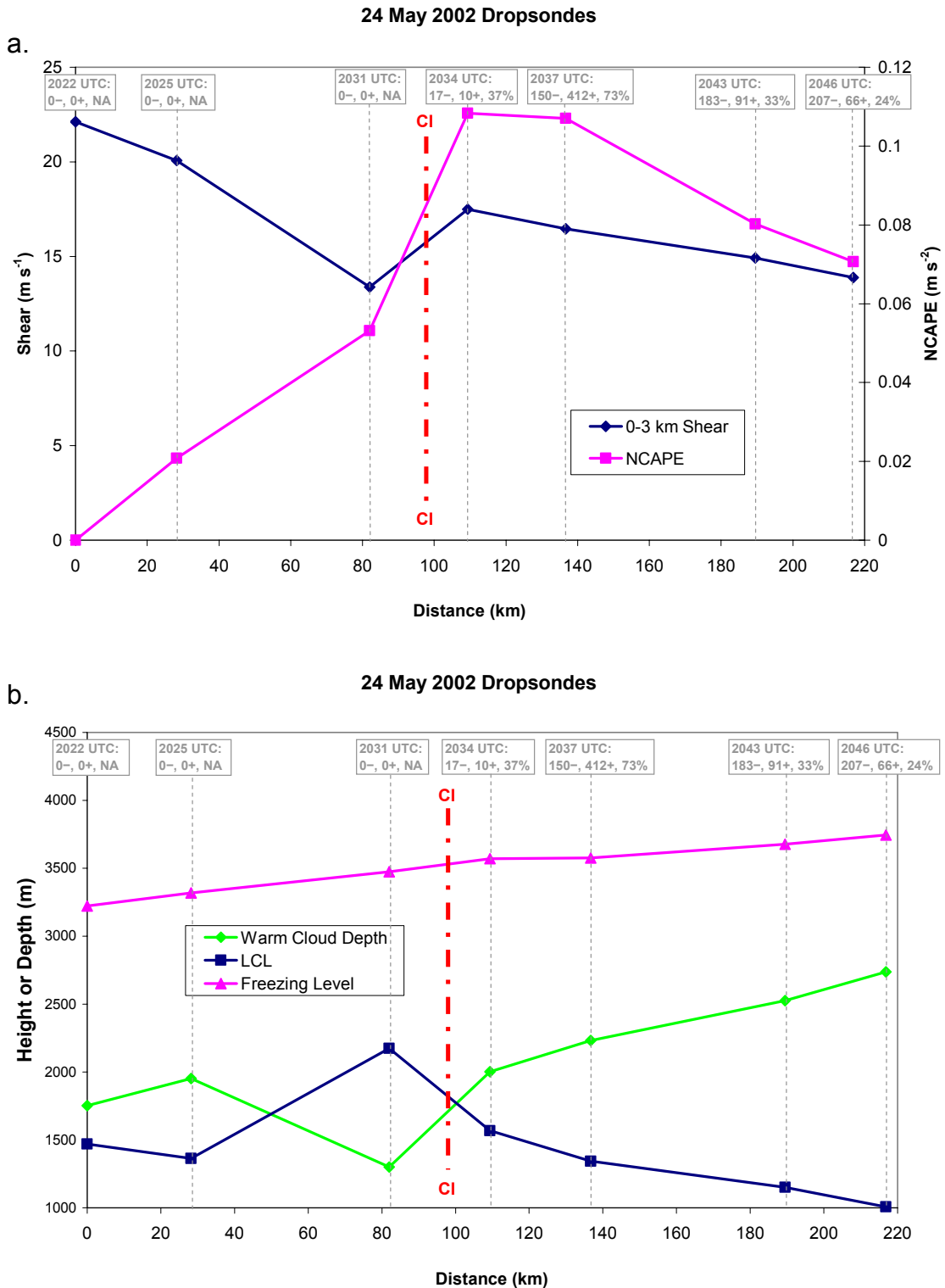
Figure 5. Sounding parameters calculated from the 24 May 2002 dropsondes as a function of distance (km) along the Learjet flight track, including **a)** low-level (0-3 km) shear (m s^{-1}) and NCAPE (m s^{-2}); **b)** warm cloud depth (m), LCL (m), and freezing level (m) above ground level. The time of each dropsonde is indicated and annotated by a dashed line. The number of negative and positive CG flashes and percent positive for storms centered about 13.7 km either side of the dropsonde location are shown. The red dash-dot line shows the location of convective initiation.
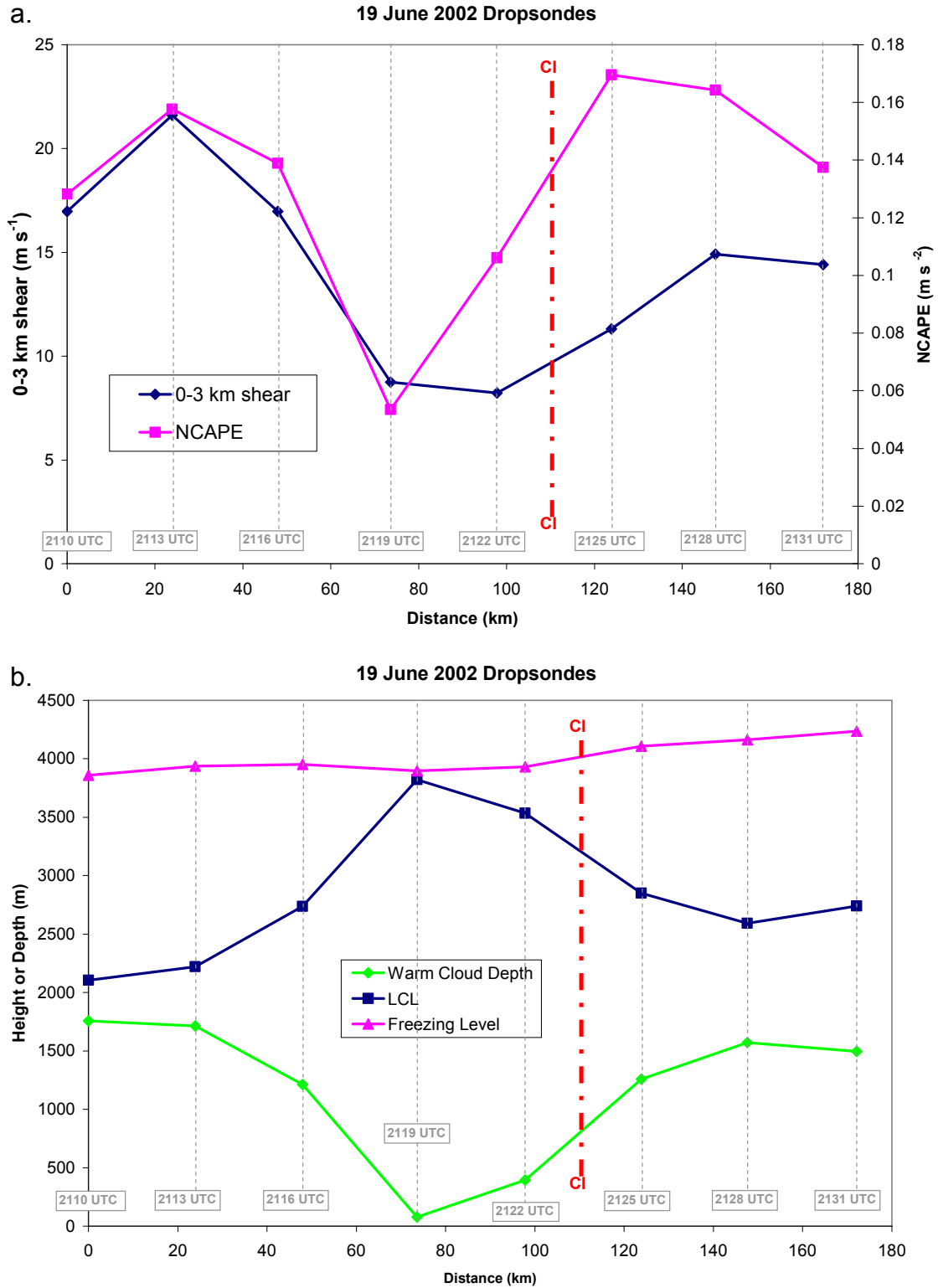
Figure 6. Same as Figure 5 except for the 19 June 2002 dropsondes. Note: The CG lightning polarity was overwhelmingly positive (~ 71.5 %) for the entire period (c.f. Figure 1b and 2b).

located at 217 km along the Learjet flight track (i.e., about 120 km eastward of where convection initiated). The height of the freezing level gradually increased eastward along the flight track. Combining the LCL and freezing level heights on 24 May in Figure 5b, the warm cloud depth increased noticeably eastward of the dryline from a value that was between 1300 m and 2000 m where convection initiated to just above 2700 m about 120 km eastward of CI. As a result, the dramatic decrease in the percentage of positive ground flashes eastward of the dryline on 24 May was accompanied by a slight increase in the freezing level, a significant lowering of the LCL, and an associated noteworthy increase in the warm cloud depth.

On 19 June 2002, the NCAPE and 0-3 km shear were at a minimum just behind (i.e., northwestward) the cold front along which CI occurred and were a maximum within 15 to 40 km ahead (southeastward) of the front (Figure 6a). Low level shear increased and then remained steady southeastward of the front while NCAPE decreased slightly at first and then more rapidly toward the end of the Learjet flight track. The peak value of NCAPE on 19 June was about 0.17 m s^{-2}, which is roughly 50% larger than for 24 May. The 0-3 km shear was generally lower on 19 June with values ranging from 10 to 15 m s^{-1}. The LCL peaked behind the cold front yet was noticeably high just ahead (southeastward) of the cold front where CI occurred (i.e., between 3550 m and 2850 m) (Figure 6b). The LCL never dropped below 2600 m in areas associated with convection on 19 June. The freezing level increased by several hundred meters southeastward (ahead) of the cold front (Figure 6b). The warm cloud depth in the vicinity of CI on 19 June was somewhere between a paltry 400 m and 1250 m and then increased toward the southeast. However, the warm cloud depth never exceeded 1600 m along the Learjet flight track on 19 June (Figure 6b), which is significantly less than the corresponding maximum warm cloud depth on 24 May.

3.3 Horizontal buoyancy, buoyancy gradients and the baroclinic generation of horizontal vorticity

Recent studies (e.g., Markowski et al. 1998; Rasmussen et al. 2000) have suggested the importance of the baroclinic or solenoidal generation of horizontal vorticity along pre-existing boundaries for tornado production in supercells. Horizontal vorticity generated in this manner can be stretched by inflow air, tilted into the vertical by the updraft, and further stretched by the updraft. Given the location of positive storms in areas of high surface θ_e gradient, Carey et al. (2003) noted that horizontal buoyancy gradients might also affect storm dynamics and hence updraft strength, cloud electrification, and lightning production in a similar manner.

To investigate the general idea and to refine the hypothesis, we present vertical cross-sections of horizontal buoyancy (B) and horizontal buoyancy gradient (dB/dH) along the Learjet flight track in the horizontal (H), which was roughly perpendicular to the surface θ_e gradient on both 24 May 2002 (Figures 7a,b) and 19 June 2002 (Figures 8a,b). On 24 May the flight

track was nearly east-west (Figure 1a) while on 19 June it was oriented from northwest to southeast (Figure 1b).
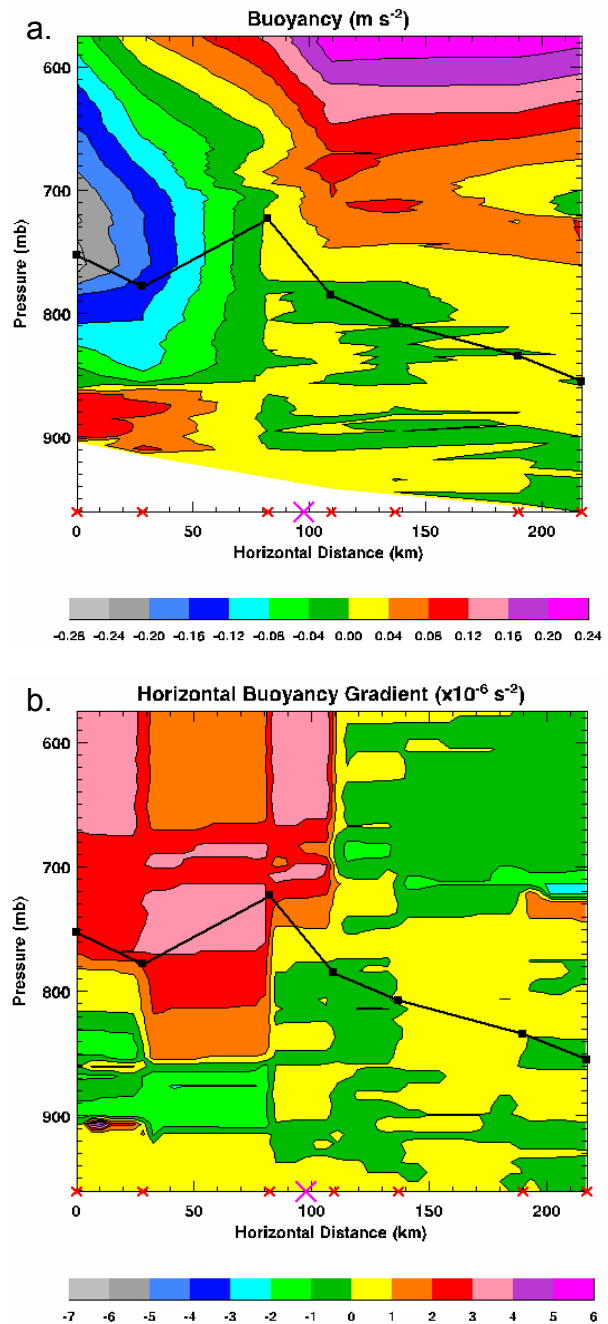
Figure 7. Vertical (pressure, hPa or mb) cross-section of the **a)** buoyancy (B, m s^{-2}) and **b)** horizontal buoyancy gradient (dB/dH, 10^{-6} s^{-2}) calculated from the dropsonde data as a function of horizontal distance along the Learjet flight track (km) on 24 May 2002. The black line indicates the LCL in mb. The large purple X marks the location of convective initiation along the Learjet flight track. The small red x's mark the dropsonde positions.

On 24 May, negative buoyancy was present in the relative cool, stable air behind the cold front (H: 0-70 km) with a minimum value between 800 and 700 mb (Figure 7a). Positive buoyancy was located eastward of the dryline (H > 70 km) at pressures less than about 800 mb with maximum values associated with the flight level pressure (~ 575 mb) of the Learjet where the dropsondes originated on 24 May. Contours of positive buoyancy sloped westward and upward in the vicinity of the dryline and cold front where CI occurred over the top of the negative buoyancy associated with stable air below (H: 40-110 km; P: 750-575 mb). Within about 10-15 km eastward of the CI, the buoyancy contours associated with the positive maximum were relatively horizontal or constant at fixed pressure. The sloped buoyancy lines associated with the dryline and cold front aloft result in a positive peak (3-4 x 10^{-6} s^{-2}) in the horizontal buoyancy gradient along the dryline/cold front boundary aloft (see upper left hand quadrant of Figure 7b), which begins at and extends above cloud base height (LCL) in the vicinity of CI.

On 19 June, the weak cold front made for a more complex pattern in the buoyancy and buoyancy gradient in the vertical (Figures 8a,b). Nonetheless, the general result in the vicinity of the cold front aloft where CI occurred is generally the same as on 24 May. A positive buoyancy maximum occurred at flight level (~475 mb) just forward (i.e., southeastward) of the cold front (H: 120-150 km) and the buoyancy was generally positive above the LCL. The buoyancy contours sloped rearward (i.e., northwestward) and upward in the vicinity of the cold front (H: 80-120 km; Figure 8a), resulting in a positive horizontal buoyancy gradient over the top of the cold front (Figure 8b) extending from cloud base upward to where the vertical cross-section terminates at flight level (P: 600-475 mb).

The two-dimensional (x-z plane) horizontal vorticity tendency equation for inviscid Boussinesq flow (neglecting Coriolis) is (e.g., Houze 1993)

$$\frac{d\xi}{dt} = -\frac{\partial B}{\partial x} \qquad (2)$$

where buoyancy (B) is defined by (1) above and ξ is the horizontal vorticity in the y-direction[1]. In this case, vorticity is generated only by a buoyancy gradient (in the x-direction). To roughly estimate the maximum amount of horizontal vorticity generated baroclinically from (2) at some pressure level, we can multiply the maximum buoyancy gradient at that level by the time the cloud resides within the buoyancy gradient.

For 24 May, the horizontal buoyancy gradient is about 3.5×10^{-6} s^{-2} (Figure 7b). The distance from the point of CI to the end of the gradient region was approximately 12 km. Based on radar, storms resided in this gradient region for about 15 min (900 sec),

[1] Note that (2) is approximately valid for 24 May since the dropsonde was oriented roughly east-to-west. For 19 June, the coordinate system would have to be rotated to be parallel to the Learjet flight track. Even so, (2) provides a rough estimate of the magnitude of the horizontal vorticity generation.

generating a horizontal vorticity of 3.15×10^{-3} s^{-1}, which is comparable to the horizontal vorticity associated with 0-3 km shear in the same region (i.e., (15.43 m s^{-1}) / (3000 m) = 5.14×10^{-3} s^{-1}).

For 19 June, the horizontal buoyancy gradient is about 5×10^{-6} s^{-2}. The distance from CI to the end of the buoyancy gradient was about 15 km. From radar, storms resided in this gradient region for approximately 20 minutes (1200 s), resulting in horizontal vorticity of 6.0×10^{-3} s^{-1}, which is comparable to the horizontal vorticity associated with 0-3 km shear in the same region (i.e., (9.78 m s^{-1}) / (3000 m) = 3.26×10^{-3} s^{-1}).
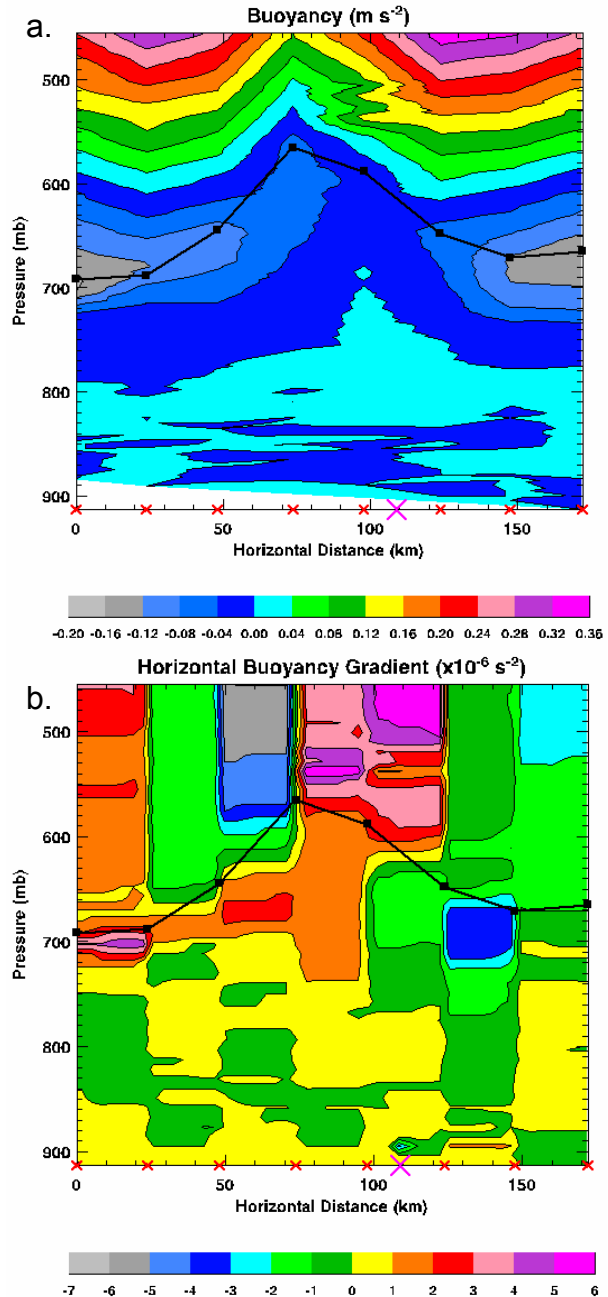

Figure 8. Same as Figure 7 except for 19 June 2002.

4. DISCUSSION AND CONCLUSIONS

Analysis of the dropsonde data from the 24 May IHOP-2002 severe storm event documented the evolution of environmental conditions associated with a storm system that underwent a transition in dominant CG lightning polarity from positive (+CG% = 73%) to negative (+CG% = 24%) as it moved eastward away from the dryline. The dramatic decrease in positive CG percentage was accompanied by significant reductions in the NCAPE and the LCL, a modest decrease in the 0-3 km shear, and a sharp increase in the warm cloud depth.

By contrast, the 19 June 2002 severe storm event generated elevated values of positive ground flash percentage during the entire system evolution over the IHOP domain (mean event +CG% = 72%). Positive storm status was associated with relatively steady peaks in the NCAPE and 0-3 km shear, elevated LCL, and correspondingly low warm cloud depth. Compared to the 24 May event, the NCAPE and LCL were substantially higher and the warm cloud depth was significantly lower on 19 June. The 0-3 km shear was comparable to slightly higher on 24 May.

Analysis of dropsonde data in the vicinity of two positive storms on 24 May and 19 June during IHOP-2002 support the earlier conclusions of Carey and Buffalo (2004). Namely, they found systematic differences between the mean environmental properties of mesoscale regions associated with positive and negative storms. In particular, positive mesoscale regions were characterized by higher LCL, smaller warm cloud depth, larger CAPE from -10°C to -40°C, larger NCAPE from LFC to -40°C, and larger 0-3 km shear. Each of these significant differences in the mesoscale environment could contribute to stronger updrafts and/or higher liquid water contents in the mixed-phase zone of positive storms.

Larger NCAPE and 0-3 km shear in positive storms would result in stronger buoyancy and dynamic forcing of the updraft and hence larger updrafts in the mixed-phase zone (e.g., Weisman and Klemp 1982; Rotunno et al. 1988). Higher LCL, and hence cloud base height, is associated with increased horizontal diameter of the buoyant parcel or horizontal eddy size. The increased diameter of the updraft associated with the higher LCL would result in less entrainment, more efficient processing of CAPE, and ultimately stronger updrafts (e.g., Lucas et al. 1996; McCaul and Cohen 2002; Williams and Stanfill 2002; Zipser 2003; Williams et al. 2004; Williams 2004). Smaller warm cloud depths would tend to suppress collision-coalescence processes (Williams et al. 2004; Williams 2004). All else being equal, warm rain processes (i.e., collision-coalescence) effectively reduces the amount of cloud water that is available in the mixed phase zone because of subsequent rainout or freezing of large rain drops. As a result, shallow warm cloud depths and the associated suppression of collision-coalescence would tend to increase the amount of supercooled cloud water available for non-inductive charging in the mixed phase zone (Williams et al. 2004; Williams 2004).

As in Carey and Rutledge (2004), we have investigated several potential controls on updraft strength and hence supercooled cloud water content: 1) buoyancy magnitude and vertical profile shape (Lucas et al. 1994; Blanchard 1998) via calculation of NCAPE, 2) dynamical forcing via estimation of shear (e.g., 0-3 km shear), and 3) cloud base height and its hypothesized effect on updraft diameter and entrainment (e.g., Williams and Stanfill 2002). We have also documented variations in the warm cloud depth, which may directly control the supercooled cloud water content through the process of coalescence and rainout (Williams et al. 2004).

In addition, baroclinic generation of horizontal vorticity was explored as another potential dynamical forcing of the updraft associated with horizontal gradients in the buoyancy (Markowski et al. 1998; Rasmussen et al. 2000; Carey et al. 2003). In the vicinity of vertically sloping surface boundaries such as a cold front or dry line, the buoyancy contours were also sloped upward and rearward over the top of the cold, dry, stable air, generating a localized maximum in the horizontal buoyancy gradient (3.5 to 5×10^{-6} s^{-2}) in the vicinity where convection typically initiated. The convection usually resided in the horizontal buoyancy gradient maximum for about 15-20 minutes (900-1200 s), resulting in horizontal vorticity production of about 3.2 to 6.0×10^{-3} s^{-1} beginning at the LCL and extending upward through mid levels in the storm (Note: nearby full vertical soundings on both days revealed a broad buoyancy maximum from about 600 mb to 200 mb with peak buoyancy values near about 400 mb). Baroclinic was comparable to shear (e.g., vertical shear of the low-level, 0-3 km, horizontal wind) generation of horizontal vorticity, and thus appears to be potentially significant. The tilting of this baroclinically generated horizontal vorticity into the vertical and subsequent stretching by an intense updraft can lead to the development of nonlinear dynamic pressure perturbations at mid-levels, and an associated dynamically accelerated updraft at low-to-mid levels in the storm (e.g., Klemp 1987). This dynamical enhancement of the low-level updraft during the developing phase of the severe convection may directly lead to elevated values of supercooled liquid water. However, since it appears to be operative during the first 15-20 minutes of the convective life cycle, the key role of a dynamically forced low-level updraft from tilted and stretched baroclinically generated horizontal vorticity may be to offset the deleterious effects of entrainment and/or precipitation loading during the formative stages of the convection.

The results presented herein and in Carey and Buffalo (2004) are generally consistent with the hypothesis that enhanced positive CG percentage in so-called positive storms is likely caused by a mesoscale environment that favors stronger updrafts and/or higher liquid water contents in the mixed phase zone, associated non-inductive positive charging of graupel and hail, and an enhanced positive charge at low-levels in the storms.

5. REFERENCES

Blanchard, D. O., 1998: Assessing the vertical distribution of Convective Available Potential Energy. *Wea. Forecasting*, **13**, 870-877.

Bluestein, H. B., 1993: *Observations and Theory of Weather Systems, Synoptic-Dynamic Meteorology in Midlatitudes.* Vol. II. Oxford University Press, 594 pp.

Branick, M. L., and C. A. Doswell III, 1992: An observation of the relationship between supercell structure and lightning ground-strike polarity. *Wea. Forecasting*, **7**, 143–149.

Carey, L. D., and S. A. Rutledge, 1998: Electrical and multiparameter radar observations of a severe hailstorm. *J. Geophys. Res.*, **103**, 13 979–14 000.

Carey, L. D., and S. A. Rutledge, 2003: Characteristics of cloud-to-ground lightning in severe and nonsevere storms over the central United States from 1989–1998. *J. Geophys. Res.*, **108**, 4483, doi:10.1029/2002JD002951.

Carey, L. D., and K. M. Buffalo, 2004: Environmental control of cloud-to-ground lightning polarity in severe storms during IHOP. *22nd Conference on Severe Local Storms*, Hyannis, MA, Amer. Meteor. Soc., paper 16B.3. Available on the Internet at http://ams.confex.com/ams/pdfpapers/81029.pdf

Carey, L. D., and S. A. Rutledge, and W. A. Petersen, 2003: The relationship between severe storm reports and cloud-to-ground lightning polarity in the contiguous United States from 1989 to 1998. *Mon. Wea. Rev.*, **131**, 1211–1228.

Craven, J. P., R. E. Jewell, and H. E. Brooks, 2002: Comparison between observed convective cloud-base heights and lifting condensation level for two different lifted parcels. *Wea. Forecasting*, **17**, 885–890.

Curran, E. B., and W. D. Rust, 1992: Positive ground flashes produced by low-precipitation thunderstorms in Oklahoma on 26 April 1984. *Mon. Wea. Rev.*, **120**, 544–553.

Doswell, C. A., III, and E. N. Rasmussen, 1994: The effect of neglecting the virtual temperature correction on CAPE calculations. *Wea. Forecasting*, **9**, 619–623.

Emanuel, K. A., 1994: *Atmospheric Convection.* Oxford University Press, 580 pp.

Gilmore, M. S., and L. J. Wicker, 2002: Influences of the local environment on supercell cloud-to-ground lightning, radar characteristics, and severe weather on 2 June 1995. *Mon. Wea. Rev.*, **130**, 2349–2372.

Klemp, J. B., 1987: Dynamics of a tornadic thunderstorm. *Annual Rev. Fluid Mech.*, **19**, 369-402.

Houze, R. A., Jr., 1993: *Cloud Dynamics.* Academic Press, 573 pp.

Lang, T. L. and co-authors, 2004: The Severe Thunderstorm Electrification and Precipitation Study. *Bull. Amer. Meteorol. Soc.*, **85**, 1107-1126.

Lucas, C., E. J. Zipser, and M. A. LeMone, 1994: Vertical velocity in oceanic convection off tropical Australia. *J. Atmos. Sci.*, **51**, 3183–3193.

Lucas, C., E. J. Zipser, and M. A. LeMone, 1996: Reply. *J. Atmos. Sci.*, **53**, 1212-1214.

MacGorman, D. R., and D. W. Burgess, 1994: Positive cloud-to-ground lightning in tornadic storms and hailstorms. *Mon. Wea. Rev.*, **122**, 1671–1697.

Markowski, P. M., E. N. Rasmussen, and J. M. Straka, 1998: The occurrence of tornadoes in supercells interacting with boundaries during VORTEX-95. *Wea. Forecasting*, **13**, 852-859.

McCaul, E. W., and C. Cohen, 2002: The impact on simulated storm structure and intensity of variations in the mixed layer and moist layer depths. *Mon. Wea. Rev.*, **130**, 1722-1748.

Rasmussen, E. N., S. Richardson, J. M. Straka, P. M. Markowski, and D. O. Blanchard, 2000: The association of significant tornadoes with a baroclinic boundary on 2 June 1995. *Mon. Wea. Rev.,* **128,** 174–191.

Reap, R. M., and D. R. MacGorman, 1989: Cloud-to-ground lightning: Climatological characteristics and relationships to model fields, radar observations, and severe local storms. *Mon. Wea. Rev.*, **117**, 518–535.

Rotunno, R., J. B. Klemp, M. L. Weisman, 1988: A theory for strong, long-lived squall lines, *J. Atmos. Sci.*, **42**, 271-292.

Saunders, C. P. R., W. D. Keith, and R. P. Mitzeva, 1991: The effect of liquid water on thunderstorm charging. *J. Geophys. Res.*, **96**, 11 007–11 017.

Smith, S. B., J. G. LaDue, and D. R. MacGorman, 2000: The relationship between cloud-to-ground lightning polarity and surface equivalent potential temperature during three tornadic outbreaks. *Mon. Wea. Rev.*, **128**, 3320–3328.

Takahashi, T., 1978: Riming electrification as a charge generation mechanism in thunderstorms. *J. Atmos. Sci.*, **35**, 1536–1548.

Weisman, M. L., and J. B. Klemp, 1982: The dependence of numerically simulated convective storms on vertical wind shear and buoyancy. *Mon. Wea. Rev.*, **110**, 504–520.

Williams, E. R., 2001: The electrification of severe storms. *Severe Convective Storms, Meteor. Monogr.*, No. 50, Amer. Meteor. Soc., 527–561.

Williams, E. R., 2004: The role of elevated cloud base height in the inverted electrical polarity of severe storms, *22nd Conference on Severe Local Storms*, Hyannis, MA, Amer. Meteor. Soc., paper 16B.4.

Williams, E. R., and S. Stanfill, 2002: The physical origin of the land-ocean contrast in lightning activity. *C. R. Physique*, **3**, 1277–1292.

Williams, E. R., V. Mushtak, D. Rosenfeld, S. Goodman, and D. Boccippio, 2004: Thermodynamic conditions favorable to superlative thunderstorm updraft, mixed phase microphysics and lightning flash rate. *J. Atmos. Res.*, in press.

Zipser, E. J., 2003: Some views on "Hot Towers" after 50 years of tropical field programs and two years of TRMM data. *Cloud Systems, Hurricanes, and the Tropical Rainfall Measuring Mission (TRMM) – A Tribute to Dr. Joanne Simpson*, *Meteor. Monogr.*, No. 51, Amer. Meteor. Soc., 49–58.